A Bidirectional Cell-to-Buffer Battery Equalizer at Boundary Conduction Mode with Constant On-Time Control

Yiqing Lu, Zhengqi Wei, and Haoyu Wang, *Senior Member, IEEE*
School of Information Science and Technology
ShanghaiTech University, Shanghai, China
Shanghai Engineering Research Center of Energy Efficient and Custiom AI IC
wanghy@shanghaitech.edu.cn

2021 IEEE Energy Conversion Congress and Exposition (ECCE) | 978-1-7281-5135-9/21/$31.00 ©2021 IEEE | DOI: 10.1109/ECCE47101.2021.9595030

***Abstract*—Conventioanl adjacent Cell-to-cell battery equalizer is flawed with long energy-flow-path between remote battery cells, which incurs low balancing speed and low energy efficiency. To cope with this issue, this paper proposes a novel Cell-to-Buffer (C2B) battery equalizer. The structure consists of a multplexer network and a bidirectional buck-boost equalizer unit. The multiplexer network selects in the battery cell to link the equalizer unit. The equalizer unit transfers the energy between cell and buffer to achieve targeted equalization. An auxiliary battery cell serves as a buffer to reduce the voltage ratio equalizer unit, which helps to simplify the equalizer unit design. In the equalizer unit, boundary conduction mode (BCM) is achieved with zero current detection (ZCD) and constant on-time control. BCM operation facilitates the zero-voltage-switching (ZVS) of MOSFETs. Instead of absolute equalization, a preset voltage tolerance range is defined to improve the balancing speed. An experimental platform to equalize between battery cell and buffer is built and tested. The function of ZCD is validated. Battery cell voltage is equalized within a preset voltage range via buffer.**

***Index Terms*—battery equalizer, boundary conduction mode, constant on-time control, multiplexer network, zero current detection**

I. Introduction

With the evolvement of energy storage technology, rechargeable battery has become the most common portable power supply [1]. Series-connected battery strings are utilized in power systems, electric vehicles or portable devices to provide readily energy. However, individual cells have mismatch in capacity, voltage rate and temperature characteristics due to the manufacturing process [2]. The discrepancy of battery parameters makes cells inconsistent in voltage or capacity, which results in battery overcharge and depletion issues [3]. Hence, the system performance is affected and even hazards of fire or explosion occur. To deal with these problems, battery management, especially battery cell equalization, is necessary [4]. The main purpose of cell equalization is to redistribute inconsistent energy between battery cells and to maintain that the entire battery string works in safe operation region. Therefore, the battery life cycle can be prolonged and risky usage can be avoided.

This work was supported in part by the National Natural Science Foundation of China under Grant 52077140, and in part by the Shanghai Rising Star Program under Grant 20QA1406700.

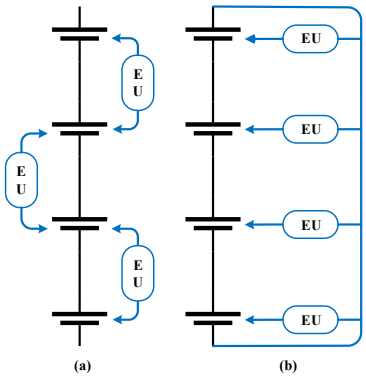

Fig. 1. Typical active equalization topologies (EU: Equalizer unit). (a) Cell-to-Cell equalization, (b) Pack-to-Cell equalization.

Different solutions of cell equalization have been proposed in recent years. The most widely used balancing method is passive equalization. A shunting resistor is parallelled with a battery cell to dissipate the excessive energy [5]. Passive equalization methods are generally simple with low cost, but suffer from zero efficiency and thermal management challenges.

To reduce energy dissipation, active equalization methods are proposed. Energy is transferred from high-energy cells to low-energy ones through equalizer units. Typical active equalization topologies can be categorized into Cell-to-Cell (C2C) methods [6]–[9] and Pack-to-Cell (P2C) methods [10]–[14]. In C2C, energy transfers between individual battery cells, as indicated in Fig. 1(a). Considering the cell voltages at both ends of equalizer units are approximately the same level, non-isolated bidirectional converter, with low components cost and high efficiency, can be utilized to realize energy transfer. In [6], simple buck-boost converter is designed to serve as the equalizer unit between adjacent battery cells. However, to achieve energy transfer between remote battery cells, the energy-flow-path is long. Thus, the balancing speed is limited. Although in [7], equalizer units are constructed between any of

two cells to realize one-cycle equalization, excessive number of equalizer units deviate from the original intention of simple circuit and control of C2C method.

In another alternative equalization topology, P2C method, balancing speed issue is addressed by targeted balancing one cell with the entire battery pack, as shown in Fig. 1(b). However, two ends of the equalizer units are connected to a single cell and the whole battery pack respectively. The mismatch of voltage requires a high step-down ratio. Therefore, isolated DC-DC converters, including resonant converters [12] or dual-active-bridge (DAB) [13], [14] are always needed in P2C equalizer unit design, which adds the circuit and control complexity.

The compromise between C2C methods and P2C methods is to use an auxiliary power supply in place of the high-voltage battery pack [15]. The auxiliary voltage source can be regarded as a buffer to temporarily store energy from high-voltage cells and to charge low-voltage cells. This Cell-to-Buffer (C2B) method can reduce the voltage ratio between the two ends of the equalizer unit. Therefore, targeted equalization and simple equalizer unit design can be both achieved simultaneously. In [15], the low-voltage (LV) bus in electric vehicle serves as the buffer. However, the LV bus, which varies from $12V$ to $14V$, is still considered high compared with one single battery cell. Therefore, n isolated DC-DC converters dedicated to each cell in a n-cell battery string, which results in high circuit complexity and hardware cost. In [16], a dual cell link topology is proposed to reduce the equalizer units by half, but still $n/2$ isolated DC-DC modules are required.

Based on the actual situation that many of the cells do not require equalization at given point of time [17], a shared equalizer unit C2B method is proposed in this paper. A multiplexer network is utilized to select target battery cell into the equalization circuit. To further simplify the equalizer unit design, an auxiliary battery is introduced to serve as the energy buffer. Therefore, both ends of the equalizer units are at similar voltage level and non-isolated DC-DC converters can be used to cut down circuit size and component cost. Due to the shared C2C equalizer unit, only one battery can be balanced at a time. To ensure balancing timeliness of the equalizer, some measures are taken to improve the balancing speed. The equalizer unit is controlled to work at predicted boundary-conduction-mode (BCM) with a preset average current. Therefore, the balancing current is constant. Compared with voltage difference based equalization methods, whose current converges as cell voltage difference gets smaller, the constant current balance can obviously accelerate the balancing. Moreover, a novel balancing concept is applied to the control scheme. It is not necessary to equalize all cells to exactly the same voltage in practical use. Upper and lower voltage boundaries can be preset, and the balance can be stopped when the battery voltage falls into this region. Therefore, a single cell does not occupy the equalizer unit for a long time and does not affect the equalization speed.

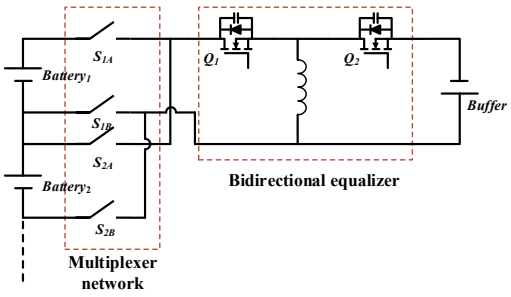

Fig. 2. Schematic of the proposed C2B equalizer

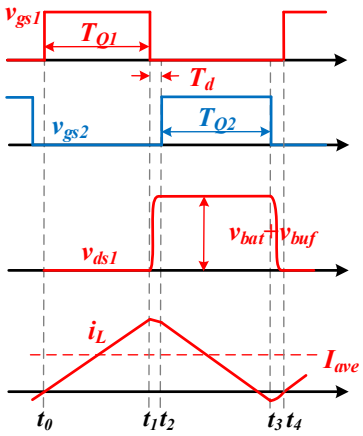

Fig. 3. Key waveforms of bidirectional equalizer unit at BCM operation.

II. Analysis of Proposed Equalizer

The schematic of the proposed equalizer is plotted in Fig. 2. It is a combination of a multiplexer network and a bidirectional buck-boost based equalizer unit. The battery cells are monitored in real-time to determine whether they are in the preset operation region. The multiplexer network selects the battery cell which needs to be balanced. The selected cell is connected to the buffer through the bidirectional buck-boost converter. The bidirectional buck-boost converter operates at BCM. A minor negative current is maintained to create the ZVS condition for the MOSFETs, which helps to reduce the switching loss.

A. Operation Principles

The shared equalizer unit means only one cell is being balanced at a specific moment. A battery cell with voltage over preset range connected to the equalizer unit is considered as an example in the analysis below. The key waveforms at BCM operation are plotted in Fig. 3. To analyze the waveforms more clearly, dead time T_d is exaggerated in the figure. The entire switching period can be divided into four sub-intervals. The current-flow of each sub-interval is exhibited in Fig. 4.

Mode I, $t \in [t_0, t_1)$, Q_1 conducts. The selected battery cell charges the inductor. Inductor current i_L increases linearly at V_{bat}/L, and reaches peak current i_{peak} at t_1. V_{Bat} stands for the voltage of the selected cell.

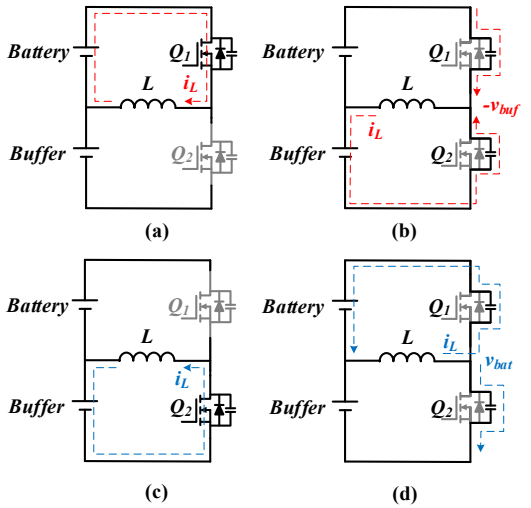

Fig. 4. The current flow of equalizer unit in four sub-intervals. (a)$t \in [t_0, t_1)$, (b)$t \in [t_1, t_2)$, (c)$t \in [t_2, t_3)$, (d)$t \in [t_3, t_4)$.

Mode II, $t \in [t_1, t_2)$, Q_1 is turned off while Q_2 remains off. The current freewheeling through the body diode of Q_2. v_{ds2} drops to zero as the large freewheels current discharges the output capacitance C_{oss} of Q_2. Therefore, ZVS condition of Q_2 is established. Meanwhile, i_L slightly varies during this period.

Mode III, $t \in [t_2, t_3)$, Q_2 conducts. The inductor releases energy to the buffer, i_L decreases linearly at $-V_{buf}/L$. V_{buf} stands for the voltage of the buffer. As to realize ZVS in the next dead band, a minor negative current $i_L(t_3)$ is needed.

Mode IV, $t \in [t_3, t_4)$, Q_2 is turned off. The minor negative current freewheels through the body diode of Q_1, discharging C_{oss} of Q_1. L resonates with the output capacitance of the MOSFETs. Therefore, v_{ds1} drops due to resonance. Since i_L is small, the rate of v_{ds1} change is slow compared with v_{ds2} during $t \in [t_1, t_2)$. The dead time T_d should be carefully designed to ensure the ZVS condition.

B. Parameters Design

During cell equalization, the voltages of selected battery cell and the buffer vary due to the energy transfer. To ensure the converter always work at BCM with variable V_{bat} and V_{buf}, a constant on-time control is adopted. As the inductor current i_L reaches 0 in every cycle at BCM operation, the peak current can be calculated according to the relationship of inductor current and voltage

$$V = L \cdot \frac{\mathrm{d}i_L}{\mathrm{d}t} \tag{1}$$

Assuming a predesigned average balancing current I_{ave}

$$i_{peak} = 2I_{ave} = \frac{V_{bat}}{L} \cdot T_{Q1} = \frac{V_{buf}}{L} \cdot T_{Q2} \tag{2}$$

according to the volt-second balance of the inductor L. The voltage of selected battery cell and buffer are known as they are monitored in real time to judge whether in preset operation region. Therefore, the conduction time of MOSFETs T_{Q1} and T_{Q2} can be calculated if L is set. Moreover, the current ripple is required to be large to realize BCM. The inductor L can also be designed smaller to compact circuit size.

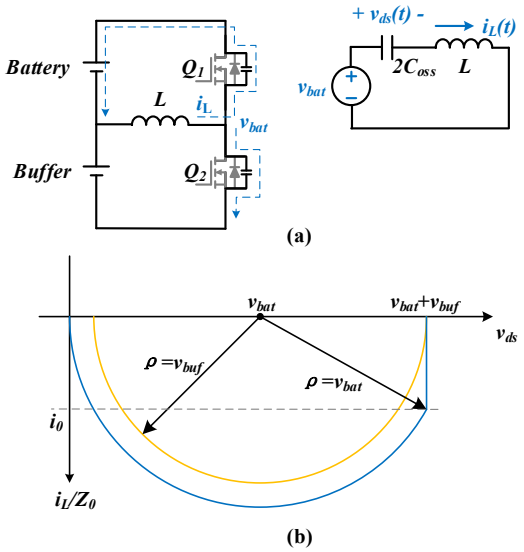

Fig. 5. ZVS analysis. (a) Equivalent circuit of equalizer unit in dead time, (b) Trajectory of ZVS analysis.

On the contrary, if the selected battery cell is undercharged, and the buffer serves as a source, the preset I_{ave} should be negative. Similar conclusion can be derived according to Equation (1) and (2).

C. Zero Voltage Switching Analysis

For power MOSFETs, turn-off loss is relatively small due to the snubber effect of output capacitance C_{oss}. Therefore, the main consideration is to migitate the current voltage overlap in the turn-on process. As mentioned, T_d is introduced to realize the ZVS of MOSFETs.

The condition of ZVS is that the inductor current can fully discharge the output capacitance of S_1 and charge the output capacitance of S_2 in Mode IV. During the dead time, C_{oss} of MOSFETs resonate with inductor L. Assuming V_{bat} and V_{buf} changes little in one switch cycle. According to KVL,

$$v_{bat}(t) \equiv V_{bat} = v_{ds1}(t) + L\frac{\mathrm{d}i_L(t)}{\mathrm{d}t} \tag{3}$$

Since C_{oss} of both MOSFETs are charged and discharged simultaneously and the equivalent circuit is derived in Fig. 5(a), where

$$i_L(t) = 2C_{oss}\frac{\mathrm{d}v_{ds}(t)}{\mathrm{d}t} \tag{4}$$

It can be derived from the Equations (3) and (4) that

$$\begin{aligned} v_{ds1}(t) &= v_{buf}cos\beta t + i_0 Z_0 sin\beta t + v_{bat} \\ i_L(t) &= -\frac{v_{buf}}{Z_0}sin\beta t + i_0 cos\beta t \end{aligned} \tag{5}$$

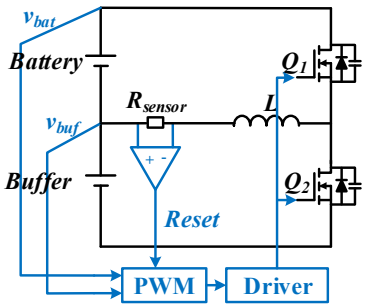

Fig. 6. Zero current detection (ZCD) to realize BCM.

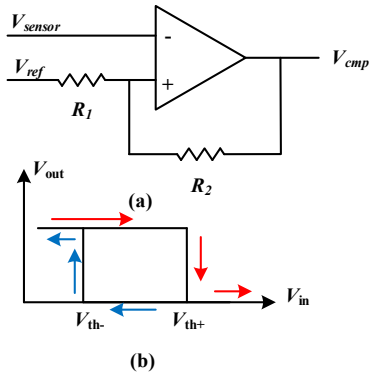

Fig. 7. ZCD method using high-speed comparator. (a) Semantic of ZCD circuit. (b) Hysteresis curve of comparator.

where

$$\beta = \sqrt{\frac{1}{2LC_{oss}}}$$
$$Z_0 = \sqrt{\frac{L}{2C_{oss}}} \tag{6}$$

and i_0 represents the negative current at t_3. The trajectory is plotted in Fig. 5(b).

It is noticed that if no negative current at t_3, v_{ds} cannot reach 0 under the assumption that $V_{bat} > V_{buf}$. That is why literally at BCM, a small negative current is actually needed. Considering the negative current i_0 can be ensured by the current variation in $t \in [t_1, t_2)$, T_d is selected smaller than half resonance period, which is

$$T_d < \frac{1}{2}\frac{2\pi}{\beta} = \pi\sqrt{2LC_{oss}} \tag{7}$$

III. Control Method

A. Zero Current Detection

The above analysis of BCM is based on the assumption that inductor current i_L starts from zero at t_0 in one switching cycle. However, T_d cannot be accurately calculated due to $i_L(t_3)$ is unknown as analyzed. The error of T_d accumulates and the balancing current finally deviates from the preset value. Therefore, to realize BCM in the whole voltage range of balancing process, inductor current needs to be monitored in real time.

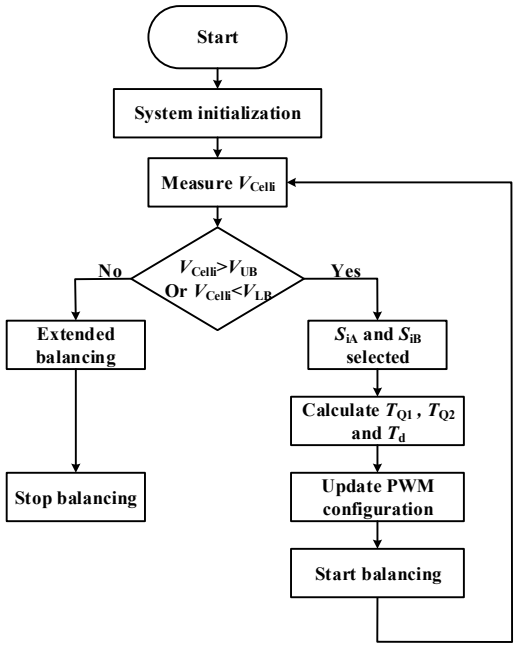

Fig. 8. The flow chart when one cell out of preset operation region is recognized and start balancing.

As the waveform suggests in Fig. 3, the crossover point of i_L is the point of time to reset PWM signal. In this paper, a zero current detection (ZCD) method is applied to control the balancing current, which is plotted in Fig. 6. A small current sampling resistance R_{sensor} is seriesly-connected to the inductor branch. The voltage drop on R_{sensor} is compared with the reference voltage V_{ref} through the high-speed comparator. V_{ref} is typically set as half of the supply voltage V_{cc} of the comparator. In ideal case, the comparison result is synchronized with the crossover point where i_L varies from negative to positive. However, in actual circuit, the time delay and the hysteresis of comparator need to be considered. Therefore, an inverse comparator is utilized in the ZCD circuit as shown in Fig. 7(a), and the threshold voltage can be derived as

$$V_{th-} = \frac{\frac{1}{2}R_2}{R_1 + R_2}V_{cc}$$
$$V_{th+} = \frac{R_1 + \frac{1}{2}R_2}{R_1 + R_2}V_{cc} \tag{8}$$

when $V_{ref} = \frac{1}{2}V_{cc}$.

According to the hysteresis curve in Fig.7 (b), the comparison result is set high voltage when i_L is slightly smaller than V_{th-}. However, the signal cannot be immediately captured by controller due to the time delay of component. The time delay is considered to let the current get more negative to ensure reliable ZVS. Then, after the preset T_d, i_L is considered to be zero and the PWM generator is reset to proceed a new switch cycle.

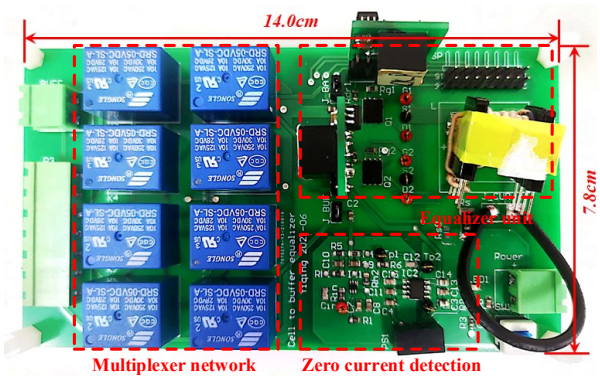

Fig. 9. Photo of the experimental prototype.

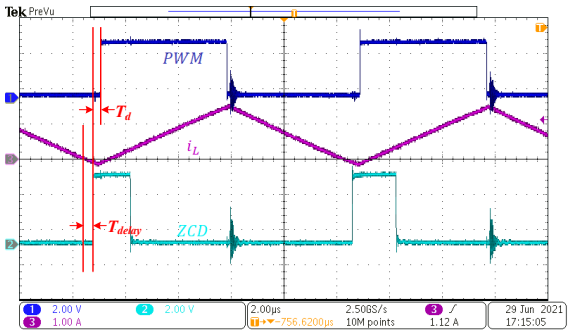

Fig. 10. Key waveforms of ZCD validation.

TABLE I: Components and main parameters of the experimental prototype

Components	Batteries	NCR18650PF
	Monitor IC	BQ76PL536
	Controller	TMS320F28379
	MOSFETs	BSC059N04LS6
	Comparator	ADCMP601
Designed parameters	Inductor L	$10\mu H$
	Output capacitance C_{oss}	$210pF$
	Average current I_{ave}	$0.75A$
	Deadband time T_d	$200ns$
	Hysteresis window V_{th}	$10mV$
	Upper bound voltage V_{UB}	$3.8V$
	Lower bound voltage V_{LB}	$3.65V$

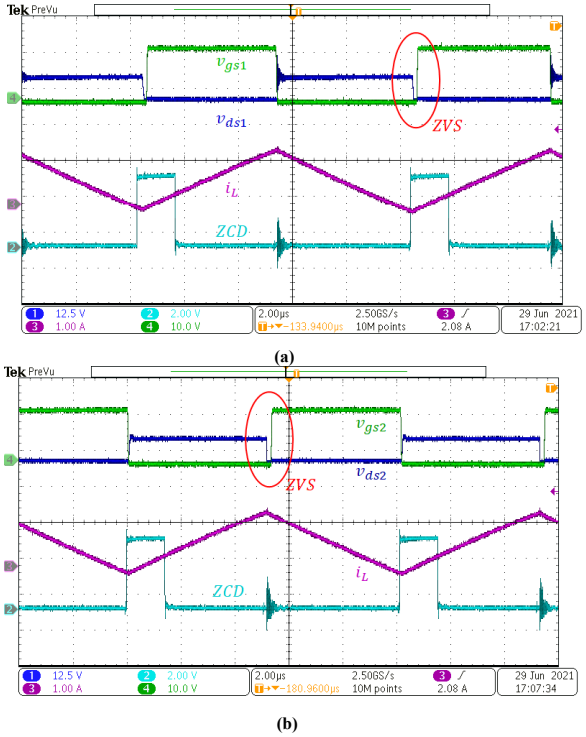

Fig. 11. Key waveforms of steady state i_L, ZCD signal and MOSFET voltage. (a) v_{gs1} and v_{ds1}, (b) v_{gs2} and v_{ds2}.

B. Control Strategy

As mentioned, to reduce balancing time and to improve timeliness, the cells are not equalized to a same specific average voltage. An operation voltage range is set with upper bound V_{UB} and lower bound V_{LB}. The voltages of battery cells and buffer are sampled in real-time by a voltage detection board. The flow chart is plotted in Fig. 8 exhibiting how the equalizer operates when one imbalance cell is recognized by voltage detection.

When the voltage of a certain cell is judged as out of the preset operation region, the balancing process is activated with a predesigned average balancing current. The correlated multiplexer network will be enabled and the selected cell is connected to the equalizer unit. The conduction time of MOSFETs T_{Q1}, T_{Q2} and the dead time T_d are calculated according to Equations (2) and (7). Equalization is at BCM operation and the ZVS of MOSFETs can be achieved. When the voltage of the selected cell returns to the preset operation region, equalization is about to end. Considering the recovery effect of battery cell, an extended balancing period is needed to compensate the self-recovery. After compensation, the multiplexer network will be turned off, until another cell needs to be balanced.

IV. Experiment Results

A. Experiment Setup

To validate the performance of the proposed equalization method, an experimental prototype to balance four series-connected battery cells is built. The photo of the prototype is shown in Fig. 9 and the parameters are listed in Table I. NCR18650PF Lithium-ion cells are utilized to construct the battery string. One auxiliary battery cell of the same type is added to the battery string to serve as a buffer. A monitor IC BQ76PL536 is utilized to sample the voltage of each cell, as well as the buffer, and transmit the acquired data to controller in real time. The multiplexer network consists of eight bidiredtional relays, which do not require isolated drivers and is easily controlled.

B. Steady State Validation

To ensure the equalizer unit operates at BCM, ZCD signal is utilized to reset the PWM driving signal of both MOSFETs.

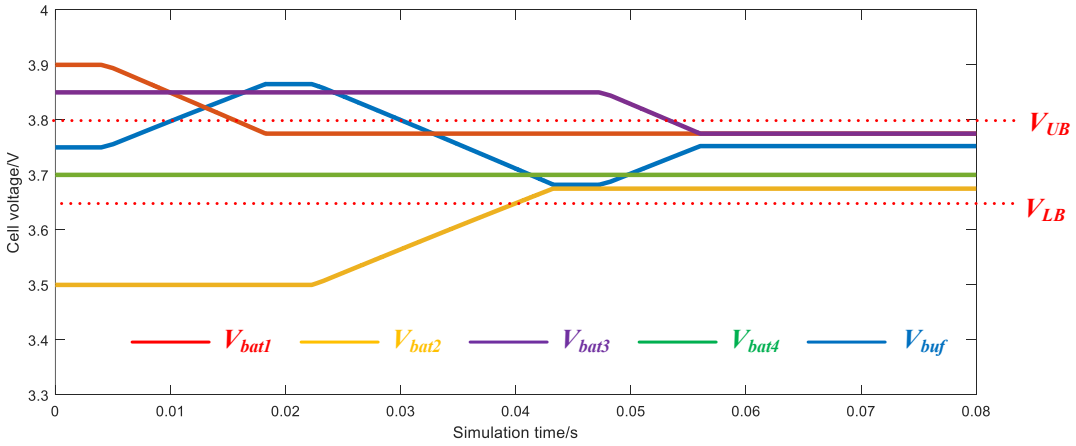

Fig. 12. Simulation result of balancing process.

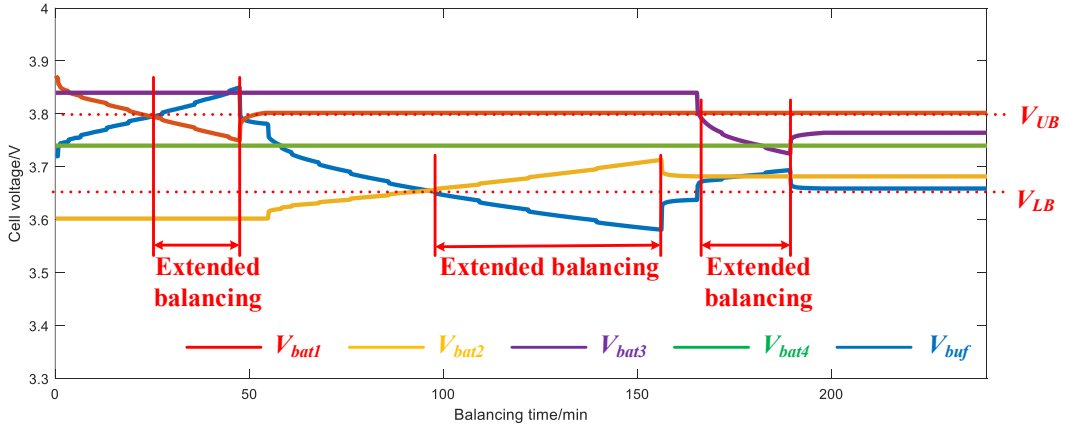

Fig. 13. Measured voltage of batteries and buffer in balancing process with manually zero current detection.

The accuracy of the ZCD signal is verified in Fig. 10. Without current control, the equalizer unit works in an open loop. It typically operates at bipolar continuous-conduction-mode (CCM), with large negative circulating current. Hence, the average balancing current degrades. In this case, the ZCD module can reset the PWM in advance, reducing the time of current drop, thus reducing the negative current. As suggested in Fig. 10, ZCD signal is set high voltage after a certain time delay when the triangular wave crosses zero to negative. The time delay $T_{delay} \approx 200ns$ according to the designed hysteresis window and the delay of component, which ensures a minor negative current to achieve ZVS. The PWM signal is reset slightly later than the ZCD signal is set high voltage, with a dead time $T_d = 200ns$ to let V_{ds} resonate to zero. Therefore, the ZVS condition is satisfied and BCM operation is also realized. There exists ringing on the ZCD signal due to the crosstalk during MOSFETs switching. However, the amplitude of the ringing is just not enough to be treated as a synchronize signal in most cases.

Fig. 11 show the steady state waveforms of inductor current and MOSFETs voltage. With the ZCD signal to reset PWM, BCM operation with a minor negative current is realized according to the inductor current. Moreover, the ZVS turn on is achieved for both MOSFETs, according to v_{gs1} and v_{ds1} in Fig. 11(a) and v_{gs2} and v_{ds2} in Fig. 11(b).

C. Balancing Process

With steady state validation, BCM operation with designed average current is realized by ZCD. Cell-to-buffer equalization with initial voltage mismatch is applied both in simualtion and in experiment. In experiment, the BCM operation is adjusted manually via monitoring the oscilloscope captured current waveform to ensure the PWM driving signal is reset when current crosses zero. Instead of constant on-time control, PWM control with fixed switching frequency is implemented. In future work, the ZCD signal can be used to automatically synchronize the driving signal and experiments with constant on-time control will be carried out. To reduce equalization time of each cell, the cells are balanced only to reach the operation voltage threshold $V_{UB} = 3.8V$ or $V_{LB} = 3.65V$. Considering the average balancing current is large, the recovery effect of battery cell is obvious. Therefore, an extended balancing is applied after the cell reaches the operation voltage boundary.

Fig.12 shows the simulation result of the balancing process. Four battery cells with initial voltage $V_{bat1} = 3.9V$, $V_{bat2} = 3.5V$, $V_{bat3} = 3.85V$ and $V_{bat4} = 3.7V$. V_{bat1} and V_{bat3} are over the upper voltage boundary, V_{bat2} is below the lower voltage boundary, and V_{bat4} falls within two boundaries. V_{buf} is initialized as a moderate value $V_{buf} = 3.75$. In simulation, ZCD signal automatically synchronizes PWM driving signal of both MOSFETs, achieving constant average current with BCM. The buffer alternately absorbs energy from the high-voltage battery cell or releases it to the low-voltage battery cell to ensure the battery voltage falls in the preset range after equalization. For battery cells with voltage already in the region, equalization is not necessarily applied. The recovery effect is not considered in simulation. Therefore, the extended balancing process is shortened, only to make balancing stop when battery voltage slightly crossover the preset boundary. The final result, as Fig.12 indicates, voltages of all four battery cells maintained in the preset region.

Fig.13 shows four battery voltage curves in the balancing process. The initial voltages of four battery cells are $V_{bat1} = 3.87V$, $V_{bat2} = 3.60V$, $V_{bat3} = 3.84V$ and $V_{bat4} = 3.74V$. Similar to simulation, the buffer voltage initiates at a moderate level and serves as a mediator to transfer energy with the high-voltage cell or low-voltage cell. The balancing starts when one cell is selected to link the equalizer unit. An extended balancing period is added after battery voltage reaches the preset boundary, until enough to compensate for the recovery effect, as exhibited in Fig.13. Then balancing stops and battery disconnects to the equalizer unit. The battery cell starts self recovery. As the recovery effect is compensated, voltage of four battery cells can finally fall in the preset region. The power of the buffer is slightly reduced due to circuit power loss. The buffer voltage may not always be distributed in the preset voltage boundary. However, the buffer is an auxiliary battery cell and not utilized as power supply. The buffer voltage does not maintain at a fixed value for very long, as power transferring between buffer and the next battery cell starts when one battery cell finishes balancing. Therefore, the buffer voltage is not limited between V_{UB} and V_{LB}, as long as it operates in the tolarable voltage range of Lithium-ion battery.

V. Conclusion

In this paper, a C2B battery equalizer structure consists of a multiplexer network and a bidirectional buck-boost equalizer unit is proposed. The equalizer unit operates at BCM with a presigned average balancing current. A ZCD module is introduced to detect the crossover point of inductor current from positive to negative. The ZCD signal can reset PWM control of both MOSFETs, which helps to achieve BCM with minor negative current in the whole voltage range while balancing. Considering the shared equalizer unit balances one cell at a point of time, the cells are balanced only to reach the tolarable operation region to accelerate the balancing. The balancing error induced by the battery recovery effect is considered and an extended balancing is applied to compensate for the error.

To evaluate the proposed concept, an experimental setup to equalize the battery string via buffer is built and tested. The ZCD signal can accurately detect the crossover point of inductor current. The equalizer operates at BCM and ZVS of both MOSFETs are realized. The battery cell voltage maintains in the preset voltage range after the energy transfer with buffer. Recovery effect is considered and compensated by an extended balancing period, which further ensures the battery voltage within preset range. The experimental results partically validate the theoretical analysis of the proposed equalizer. In future work, the ZCD module will be applied to synchronize the driving signal, and automatically constant on-time will be validated.

References

[1] S. Yarlagadda, T. T. Hartley, and I. Husain, "A battery management system using an active charge equalization technique based on a dc/dc converter topology," *IEEE Trans. Ind. Appl.*, vol. 49, no. 6, pp. 2720–2729, 2013.

[2] W. Diao, N. Xue, V. Bhattacharjee, J. Jiang, O. Karabasoglu, and M. Pecht, "Active battery cell equalization based on residual available energy maximization," *Appl. Energy*, vol. 210, pp. 690–698, 2018.

[3] F. Peng, H. Wang, and Z. Wei, "An llc-based highly efficient s2m and c2c hybrid hierarchical battery equalizer," *IEEE Trans. Power Electron.*, vol. 35, no. 6, pp. 5928–5937, 2019.

[4] F. Feng, X. Hu, J. Liu, X. Lin, and B. Liu, "A review of equalization strategies for series battery packs: variables, objectives, and algorithms," *Renew. Sust. Energ. Rev.*, vol. 116, p. 109464, 2019.

[5] J. Gallardo-Lozano, E. Romero-Cadaval, M. I. Milanes-Montero, and M. A. Guerrero-Martinez, "Battery equalization active methods," *J. Power Sources*, vol. 246, pp. 934–949, 2014.

[6] T. H. Phung, A. Collet, and J.-C. Crebier, "An Optimized Topology for Next-to-Next Balancing of Series-Connected Lithium-ion Cells," *IEEE Trans. Power Electron.*, vol. 29, no. 9, pp. 4603–4613, 2014.

[7] F. Mestrallet, L. Kerachev, J.-C. Crebier, and A. Collet, "Multiphase interleaved converter for lithium battery active balancing," *IEEE Trans. Power Electron.*, vol. 29, no. 6, pp. 2874–2881, 2013.

[8] F. Peng, H. Wang, and L. Yu, "Analysis and design considerations of efficiency enhanced hierarchical battery equalizer based on bipolar ccm buck–boost units," *IEEE Trans. Ind. Appl.*, vol. 55, no. 4, pp. 4053–4063, 2019.

[9] X. Ding, D. Zhang, J. Cheng, B. Wang, Y. Chai, Z. Zhao, R. Xiong, and P. C. K. Luk, "A novel active equalization topology for series-connected lithium-ion battery packs," *IEEE Trans. Ind. Appl.*, vol. 56, no. 6, pp. 6892–6903, 2020.

[10] M. Einhorn, W. Roessler, and J. Fleig, "Improved performance of serially connected li-ion batteries with active cell balancing in electric vehicles," *IEEE Trans. Veh. Technol.*, vol. 60, no. 6, pp. 2448–2457, 2011.

[11] M. Uno and K. Tanaka, "Single-switch cell voltage equalizer using multistacked buck-boost converters operating in discontinuous conduction mode for series-connected energy storage cells," *IEEE Trans. Veh. Technol.*, vol. 60, no. 8, pp. 3635–3645, 2011.

[12] M. Uno and A. Kukita, "Bidirectional pwm converter integrating cell voltage equalizer using series-resonant voltage multiplier for series-connected energy storage cells," *IEEE Trans. Power Electron.*, vol. 30, no. 6, pp. 3077–3090, 2014.

[13] J. Lu, Y. Wang, and X. Li, "Isolated bidirectional dc–dc converter with quasi-resonant zero-voltage switching for battery charge equalization," *IEEE Trans. Power Electron.*, vol. 34, no. 5, pp. 4388–4406, 2018.

[14] X. Qi, Y. Wang, and M. Fang, "An integrated cascade structure-based isolated bidirectional dc–dc converter for battery charge equalization," *IEEE Trans. Power Electron.*, vol. 35, no. 11, pp. 12 003–12 021, 2020.

[15] M. Evzelman, M. M. U. Rehman, K. Hathaway, R. Zane, D. Costinett, and D. Maksimovic, "Active balancing system for electric vehicles with incorporated low-voltage bus," *IEEE Trans. Power Electron.*, vol. 31, no. 11, pp. 7887–7895, 2015.

[16] W. Wang and M. Preindl, "Dual cell links for battery-balancing auxiliary power modules: A cost-effective increase of accessible pack capacity," *IEEE Trans. Ind. Appl.*, vol. 56, no. 2, pp. 1752–1765, 2019.
[17] S. K. Dam and V. John, "Low-frequency selection switch based cell-to-cell battery voltage equalizer with reduced switch count," *IEEE Trans. Ind. Appl.*, 2021.